INTERNATIONAL JOURNAL OF INTEGRATED ENGINEERING
ISSN: 2229-838X e-ISSN: 2600-7916

IJIE

Vol. 17 No. 8 (2025) 89-99
https://publisher.uthm.edu.my/ojs/index.php/ijie

3D Printed Tuneable Silicone Foams via Direct Templating Approach

Kenrick Weiting Tie[1], Jia Huey Sim[2,3,4]*, Purani Mohana Sundaram[2], Jing Yuen Tey[1,4], Wei Hong Yeo[1,4], Zhi Hua Lee[2,3], Law Yong Ng[2,3]

[1] *Department of Mechanical and Material Engineering, Lee Kong Chian Faculty of Engineering and Science, Universiti Tunku Abdul Rahman, Selangor, 43000, MALAYSIA*
[2] *Department of Chemical Engineering, Lee Kong Chian Faculty of Engineering and Science, Universiti Tunku Abdul Rahman, Selangor, 43000, MALAYSIA*
[3] *Centre for Photonics and Advanced Materials Research (CPAMR), Universiti Tunku Abdul Rahman, Selangor, 43000, MALAYSIA*
[4] *Centre for Sustainable Mobility Technologies (CSMT), Universiti Tunku Abdul Rahman, Selangor, 43000, MALAYSIA*

*Corresponding Author: simjh@utar.edu.my
DOI: https://doi.org/10.30880/ijie.2025.17.08.009

Article Info

Received: 25 April 2025
Accepted: 27 November 2025
Available online: 31 December 2025

Keywords

3D printing, silicone, templating, porous

Abstract

Silicone is well-known for its appealing properties like high elasticity, hydrophobicity and biocompatibility, which translates to diverse applications including silicone foams. However, current foaming methods are complex, lengthy and involves hazardous chemicals. The direct templating approach tackles these complications by saturating the silicone precursors with sacrificial templates, e.g. salts or sugar crystals. These templates are leached out in appropriate solvents after vulcanization, leaving behind porous structures. The resulting pores and mechanical properties of the foams can be tuned by varying the quantity of sacrificial templates introduced. In addition, 3D printed architectures present greater degree of complexity for said silicone foams. Herein, facile silicone foams with tuneable properties are fabricated via Direct Ink Writing (DIW) with the inclusion of glucose sugar crystals into a one-part room temperature vulcanizing (RTV-1) silicone formulation, with deionized water as the eco-friendly solvent. The silicone ink formulations were proven to fulfil viscoelastic requirements of DIW. Pore morphologies of formulated foams with varied glucose content of 15 phr to 55 phr were characterized by SEM. The results showed presence of macropores with pore sizes ranging from 26.44 µm to 52.39 µm and porosity ranging from 15.03 % to 31.60 %. The pore size and porosity of the foam samples were found to be linearly proportional to the amount of glucose content. Tensile tests unveiled that with increasing sugar content, mechanical properties of said foams had been varied with tensile strength (0.96-0.59 MPa), elongation at break (511-362 %), and Young's modulus (0.50-0.37 MPa). The foams also displayed decreasing Shore A hardness (35.8-30.1) as porosity increased. This simplistic approach represents a feasible method of creating silicone foams with tuneable properties using easily attainable and safe materials.

1. Introduction

Silicone is a polymeric material consisting of silicon, oxygen, carbon, and hydrogen, with the prevalent monomer being polydimethylsiloxane (PDMS) [1]. The Si-O bonds with high bond energy that constructs the polymer backbone facilitate its unique material properties such as excellent chemical and thermal stability, biocompatibility, high elasticity, flexibility and hydrophobicity [2]. For instance, due to its soft and biocompatible nature, silicone has been utilized in the biomedical domain for prosthesis or soft robotics [3]. Besides that, silicone products such as sealants and dampers have found applications in various industries especially in automotive and construction as the silicone material famous for its thermal stability and elasticity [4].

Recently, porous PDMS foams have been developed due to its softer, higher elasticity and porous properties compared with nonporous PDMS materials [5]. Initially, porous PDMS were developed as membranes for filtration, oil/water separation or even gas purification [6]. The separation characteristics of said membranes are reliant on its pore properties. Besides that, porous PDMS were also reported to be incorporated into tissue engineering in the form of scaffolds [7]. The PDMS-based scaffolds with three-dimensional porous network possess chemical stability and biocompatible behaviours, able to support and facilitate cell growth as well as tissue development. In more recent times, porous PDMS structures with soft and elastic characteristics have been adopted as wearable devices and sensors [8]. The stretchability and robustness of porous PDMS drive its use for pressure sensors, by measuring the capacitance or resistance changes when mechanical forces are applied on the porous PDMS based sensors [9], [10].

Owing to the characteristics of silicone polymers, they have been exploited in the foam industry [11]. Chemical and physical foaming techniques are available to fabricate silicone foams with different porosities. However, such techniques often incorporate complex machineries or hazardous chemicals to introduce the formation of pores. For instance, as an example of physical foaming, carbon dioxide (CO_2) foaming involves the injection and saturation of CO2 gas into the silicone precursor in its liquid or partially-crosslinked state at high pressures until crosslinking is completed. For chemical foaming, harmful chemical blowing agents or corrosive acid/carbonate systems are blended into the polymer which releases gaseous products while being crosslinked simultaneously. Both gas and chemical foaming methods necessitate the use of heavy machineries and toxic chemicals at times.

The direct templating approach provides a simplistic yet safe alternative to construct porous silicone foams. It involves encapsulating porogens or a sacrificial template into the silicone precursors followed by solvent extraction which leaches out this template, leaving behind a porous structure [12]. Porous silicone foams have been fabricated with this method by incorporating common and inexpensive materials such as sugar, salt or even citric acid monohydrate particles which were used as purchased [13]. Environmentally-friendly solvents such as deionized water and ethanol are proven effective to extract and dissolve these particles. Moreover, the foam properties such as the degree of porosity and pores' sizes are dependent on the size and number of particles added. Hence, this technique benefits from its low-cost versatility while foams with tuneable properties can be produced rapidly.

With additive manufacturing or 3D printing being focused on heavily as of late, parts are manufactured directly from computer-aided-design models in a layered manner [1]. The conventional silicone products are often limited to moulding or casting manufacturing processes due to the molten state and long curing duration of silicone precursors, which limits its potential for advanced applications [5], [14]. With additive manufacturing, soft and stretchable functional silicone parts can be fabricated rapidly, with minimized waste, while allowing for intricate structures with geometrical freedom for applications such as soft actuators or wearable sensors [3], [15]. Among the types of 3D printing processes used for silicone printing, Direct Ink Writing (DIW) is favoured due to its versatility [16]. DIW transpires to be a material extrusion process that dispenses a thixotropic ink through a nozzle via applied pressure in a layered-manner [17]. Objects are 3D printed from continuous filaments that are directly extruded from the nozzle and stacked layer-by-layer without any post-processing, thus making it a straightforward process. For successful printing with a DIW printer, it is imperative for viscoelastic silicone inks to exhibit certain rheological characteristics. Generally, such inks have to display rheological behaviours of having: (i) shear-thinning characteristic to permit material extrusion through a nozzle smoothly at desired flowrate; and (ii) adequate yield stress to maintain shape fidelity without sagging once exiting the nozzle [17], [18].

This study aims to fabricate low-cost porous silicone foams with tuneable properties by direct templating and DIW. Glucose particles are mechanically mixed into a silicone blend and then 3D printed. Porous silicone foams obtained from glucose/PDMS inks with different glucose loading were characterized to validate the relationship between glucose loading and properties of silicone foams. To the best of the authors' knowledge, this represents the novel study upon introducing glucose particles as the template to generate porous silicone foams via DIW.

Int. Journal of Integrated Engineering Vol. 17 No. 8 (2025) p. 89-99

2. Methodology

2.1 Materials

An RTV-1 silicone formulation with appropriate thixotropic behaviour was chosen from SiSiB® Silicones. The silicone polymer backbone employed was α, ω-silanol-terminated PDMS that has a viscosity value of 20,000 cPs. To constitute a neutral-cure silicone formulation, methyltris(methylethylketoxime) (MOS) silane and vinyl tris(methylethylketoximino) (VOS) silane oxime crosslinkers were adopted. Dibutyltin dilaurate (DBTL) served as the catalyst. Fumed nanosilica powder with a BET surface area of 100 m^2/g and silicone oil were utilized as the rheology enhancers. Glucose particles (Glucolin) from Reckitt Benckiser were used as purchased as the sugar template.

2.2 Preparation of Porous Silicone Samples

The parts per hundred rubber (phr) ratio of the silicone blend with PDMS: silicone oil: MOS: VOS: nanosilica: DBTL at 100: 16.23: 10.80: 1.20: 8.33: 0.07 respectively were kept constant. Three different silicone formulation with glucose content at 15, 35 and 55 phr respectively were prepared. Glucose particles were dispersed into the silicone blend via an overhead mixer at 300 RPM for 5 minutes to ensure homogeneous distribution. After 3D printing of the formulated silicone, the samples were immersed in deionized water at 60 °C for solvent extraction of the glucose templates in order to attain porous silicone foams.

2.3 Characterization of Rheological, Morphological, and Mechanical Properties

Rheology characterization of all inks was performed via an Anton Paar Physica MCR 301 Rheometer. Storage modulus (G') and loss modulus (G'') measurements were taken via oscillatory amplitude sweeps ranging from 0.01 to 100 % and shear strain at a constant angular frequency of 10 $rad \cdot s^{-1}$. Viscosity tests were conducted with shear rates from 0.1 to 100 s-1.

Morphology of silicone foams was observed with a Hitachi S-3400N Scanning Electron Microscope (SEM). Acceleration voltage and probe current were set at 15.0 kV and 40 mA respectively. Samples were gold coated prior to imaging. Statistical analysis was done with ImageJ application to obtain the average pore size, pore size distribution, as well as porosity from SEM images, while the porosity of the sample was evaluated based on Eq. (1) [19].

$$Porosity = \frac{Sum\ of\ pore\ area}{Total\ area\ of\ SEM\ image} \quad (1)$$

Mechanical performance of the silicone samples was evaluated by a Shimadzu AGS-kNX universal tensile testing machine. Tensile tests were carried out according to ASTM D412 type-C standard. Multiple tests were run and the average readings were plotted into stress-strain curves. Hardness values of the samples were measured with a Shore A durometer from CONIC. 5 readings were taken at arbitrary points for each sample and the average hardness values were reported.

2.4 Three-Dimensional Printing

Printing of silicone samples was done via a DIW printer. Inks were loaded into syringes, and extruded onto the printing platform via a lead-screw driven by a stepper motor. The printing parameters were kept constant with nozzle size of 0.84 mm and printing speed of 10 $mm \cdot s^{-1}$.

3. Results

3.1 Rheological Properties

The rheological parameters of the prepared glucose/PDMS inks are summarised in Table 1. From Fig. 1(a), all silicone inks showed shear-dependent behaviour. This was proven with the drop in viscosity with increasing shear rate, facilitating flow through the printing nozzle at higher shear rates. Higher glucose loading had led to inks with higher viscosities as well. At the printing shear rate of 30.32 s-1 with the printing parameters used, the increased glucose content of 15, 35 and 55 phr displayed viscosities of 62.41 Pa·s, 73.65 Pa·s, and 109.66 Pa·s respectively. This concurs with Teoh et al. [20] and Victoria et al. [21] as the larger quantity of glucose particles increased particle-particle interactions which resulted in particle agglomerates that hindered material flow. Larger shear stresses were needed to overcome the increased frictional forces.

Table 1 *Rheological properties of glucose/PDMS inks formulations*

Glucose content (phr)	Viscosity (Pa·s)	Storage modulus of LVR, G'_{LVR} (Pa)	Static yield stress, σ_y (Pa)	Loss factor at LVR, tan δ
15	62.41	4596.03	120.04	0.46
35	73.65	8072.76	132.99	0.38
55	109.66	12932.23	135.68	0.37

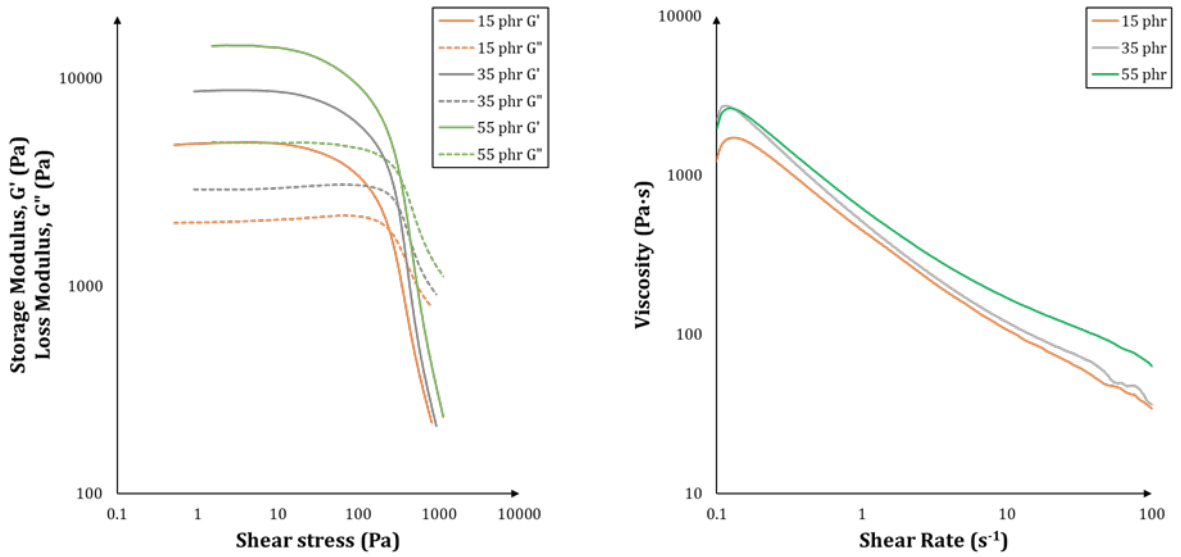

Fig. 1 *Rheological studies of glucose/PDMS inks with various glucose content for (a) Storage and loss moduli; (b) Viscosity*

The parameters of storage modulus (G') and loss modulus (G'') describe the viscoelastic behaviour of the sample, which measure the elastic and viscous response of a sample respectively [22]. The loss factor or also known as tan δ, is the ratio of G'' to G' which aids to identify at which point does a viscoelastic sample manifests solid or liquid like behaviour [23]. The sample is said to resemble a solid when $G' > G''$ (tan $\delta < 1$), while the reverse is true as the sample mimics a liquid when $G'' > G'$ (tan $\delta > 1$) [18]. The Linear Viscoelastic Region (LVR) is defined as the region where G' remains relatively constant (plateau) even with increasing amplitude, and the storage modulus at this region is termed as G'_{LVR}. According to ASTM D7175 standards, when there is a 10 % plunge in G' from this plateau, the corresponding shear stress is defined as static yield stress, σ_y of the ink [24].

It is evident from Fig. 1(b) that all ink formulations showed the criteria of $G' > G''$ in the LVR with the tan $\delta <$ 1, signifying that the inks flowed as an elastic solid rather than a viscous liquid at rest which promotes shape retention during printing [22]. The optimal loss factor values for printable inks are highly specific for a material and printing system used. M'Barki et al. [18] had reported the loss factor values between 0.1 to 0.3, while Cheng et al. [25] highlighted values between 0.2 to 0.7. Hence, the loss factor of 0.37 to 0.46 for the inks in this study aligned with values reported in literature. Next, the increased glucose loading had enhanced the storage modulus, G'_{LVR} from 4596.03 Pa to 12932.23 Pa. This can be explained as more glucose particles provided greater reinforcement which caused an increase in elastic behaviour of the RTV-1 silicone formulation [5].

Moreover, the increase in G" with higher glucose content is expected as more energy dissipation was induced by increased friction among glucose agglomerates [26]. The storage modulus values obtained in this current study (4596.03 Pa to 12932.23 Pa) were comparable to those declared by Tang et al. [27] (103 Pa to 105 Pa) and Liao et al. [28] (103 Pa to 106 Pa) for their printable silicone elastomer inks. Subsequently, printable inks have to possess sufficient yield stress for shape retention during printing [29]. The yield stress for printable silicone inks ranges from 102 Pa to 103 Pa as claimed by Lyu et al. [30], while 90 Pa was already adequate for printing according to Perrinet et al. [31]. Thus, the static yield stress values of the glucose/PDMS inks obtained in the current study were above 100 Pa which allowed for printing, while the increased glucose content led to the rise from 120.04 Pa to 135.68 Pa. This is associated with glucose particles being rigid, thus resisting deformation and limiting shear in the system which ultimately enhances yield strength [32].

Int. Journal of Integrated Engineering Vol. 17 No. 8 (2025) p. 89-99

3.2 Pore Properties

The feasibility of the direct templating method to synthesize porous silicone was verified by the presence of pores in the PDMS matrix as observed via SEM images. Elliptical closed-cell pores identical to the shape of glucose particles were apparent in all samples illustrated in Fig. 2. The pore properties were assessed with the D_{10}, D_{50}, D_{90} (pore diameter at the 10th, 50th, and 90th percentile from the cumulative relative frequency curve in Fig. 3), average pore diameter and porosity as tabulated in Table 2.

Table 2 *Pore properties of different foam samples*

Glucose content (phr)	D_{10} (μm)	D_{50} (μm)	D_{90} (μm)	Average pore diameter (μm)	Porosity (%)
15	9.00	17.00	61.77	26.44	15.03
35	12.00	28.54	67.00	35.07	26.47
55	18.00	44.00	106.85	52.39	31.60

The glucose particles acted as porogens for the direct templating technique used. From the studies on silicone foam formation via direct templating and moulding, Sanderson et al. [33] attained pore sizes of 30 μm to 100 μm. When common sugar cubes were used, González-Rivera et al. [13] recorded pores of 500 ± 300 μm, while Pandey et al. [34] declared values of 200 μm to 300 μm. However, the resulting pores from all samples templated with glucose particles in this study were relatively small, which had pore diameters between 26.44 μm to 52.39 μm, and may be classified as macropores as their average pore diameters were larger than 50 nm [6]. The small pore sizes created in the current study are specifically desired for 3D printing of silicone foam due to the fact that silicone ink embedded with larger sugar cubes (> 100 μm) tend to clog the tiny printing nozzle head, subsequently hindering from printing. From Fig. 2, the number of elliptical pores perceived were more prominent at higher glucose content. The pore properties are reliant on the concentration of the porogen introduced [35]. Hence, the increment of average pore diameters was a result of increased glucose loading from 15 phr to 55 phr with a higher tendency for particle agglomeration. This eventually produced closed-cell porous silicone foams with their porosities ranging from 15.03 % to 31.60 %.

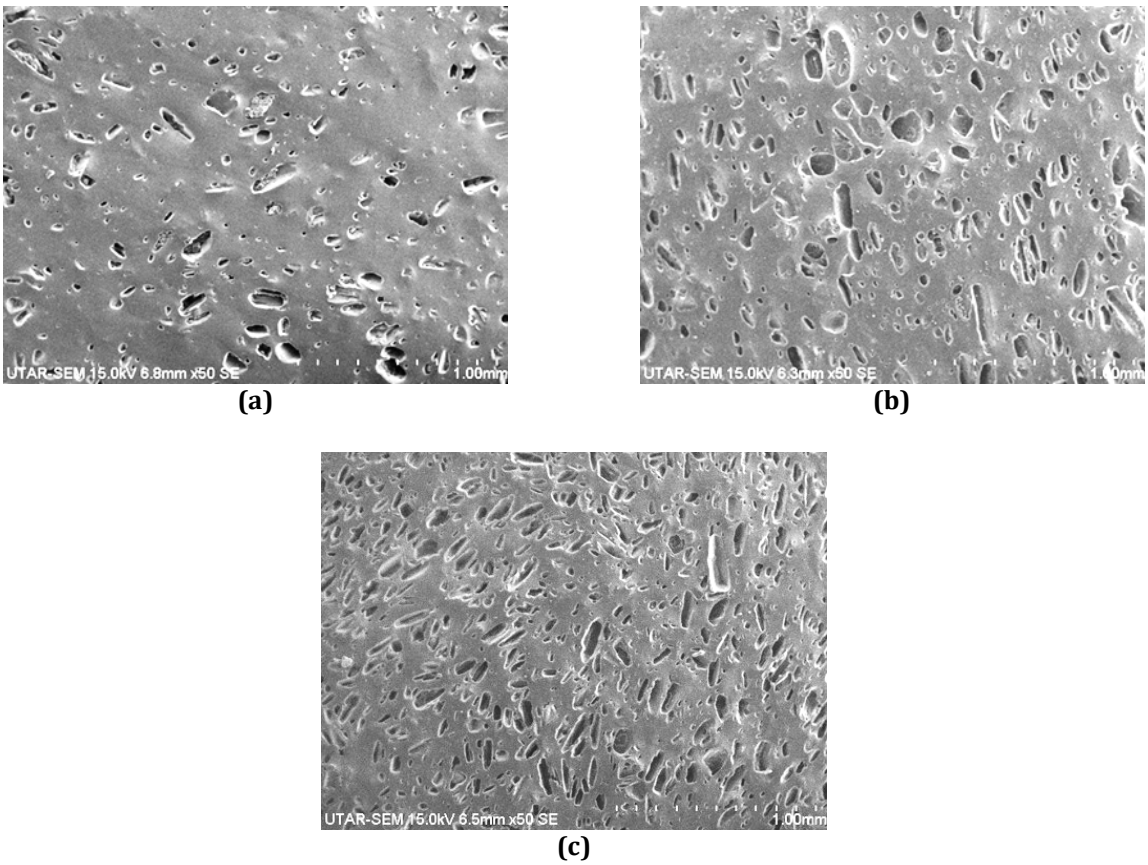

Fig. 2 *SEM images of foam samples with different glucose content of (a) 15 phr; (b) 35 phr; (c) 55 phr*

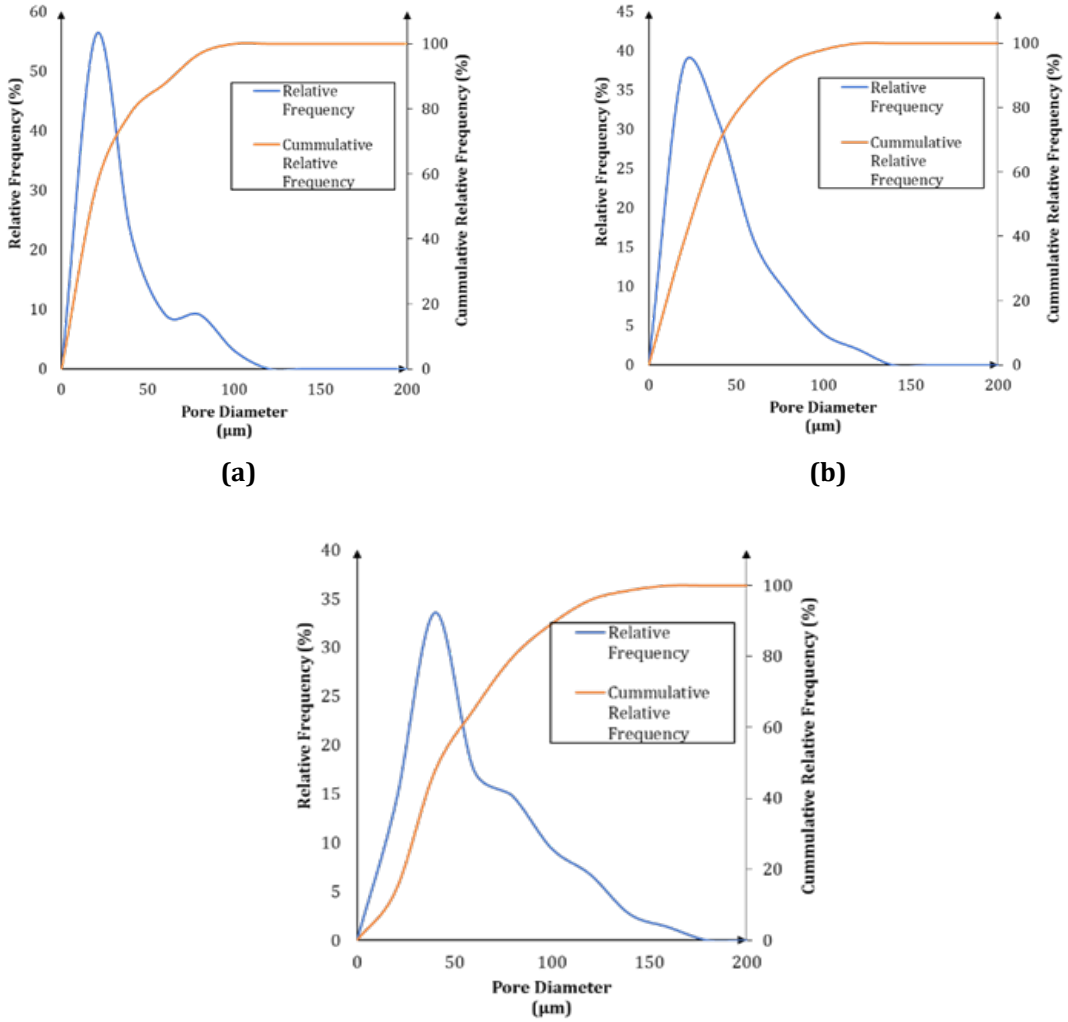

Fig. 3 *Pore size distribution curves of different foam samples at different glucose content of (a) 15 phr; (b) 35 phr; (c) 55 phr*

Linear regression in Fig. 4 illustrates that the relationship between the glucose content and average pore size, as well as porosity. The average pore size and porosity are presumed to be linearly dependent to the glucose content. High R^2 values of 0.9706 and 0.9694 were attained respectively, suggesting a strong linear correlation between glucose content with the average pore size and porosity respectively. Open-cell foams were not witnessed in all three samples, which suggested that the amount of glucose introduced into the PDMS matrix were insufficient to acquire interconnected pores [36].

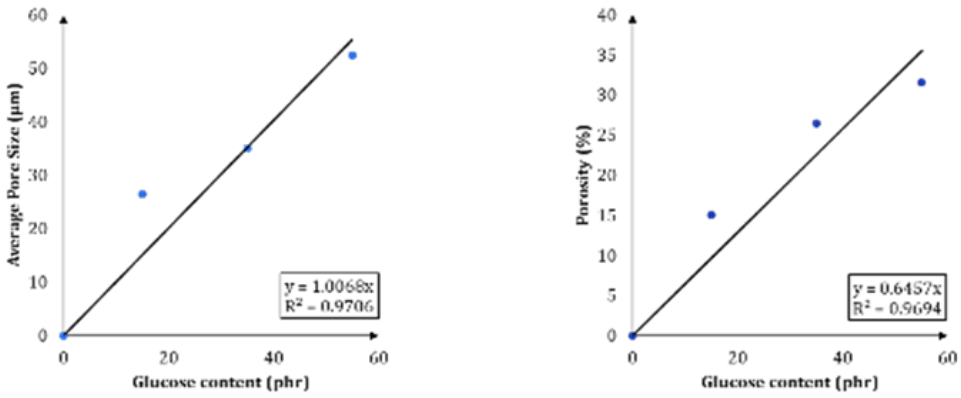

Fig. 4 *Correlation between glucose content and (a) Average pore size; (b) Porosity*

Int. Journal of Integrated Engineering Vol. 17 No. 8 (2025) p. 89-99

3.3 Mechanical Properties

Tensile tests of various porous silicone foams were carried out to establish the correlation between the pore properties with the mechanical properties The stress-strain curves in Fig. 5 showing a decreased in mechanical properties of Young's modulus, ultimate tensile strength, elongation at break with the increased of pores density. This trend agrees with the study from [37] which asserted that higher porosities generally result in lower mechanical properties for PDMS samples. The formation of pores or pores density heavily dependent on the glucose content in the ink formulation via direct templating approach. Thus, the mechanical properties of silicone foams can be customized with precise tuning of glucose content.

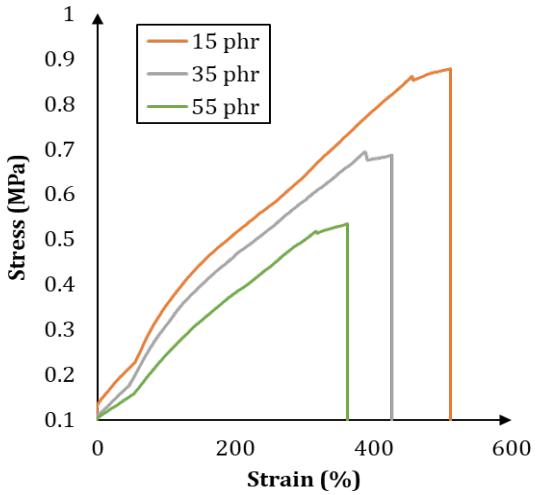

Fig. 5 *Stress-strain curves of different foam samples with different glucose content*

From Table 3, silicone foam with the smallest average pore diameter of 26.44 µm and 15.03 % porosity, resulted from 15 phr glucose added, had a Young's modulus of 0.50 MPa and ultimate tensile strength of 0.96 MPa. In contrast, silicone foam with 55 phr glucose added, had the lowest Young's modulus and ultimate tensile strength of 0.37 MPa and 0.59 MPa respectively, while having the largest pore diameter of 52.39 µm and 31.60 % porosity. This implies that as more pores were induced, the volume of PDMS matrix available for load bearing was lowered while the bulk material suffered from increased inhomogeneity, thus effectively reducing tensile strength and material stiffness [5]. All the silicone foams offered good elongation at break, with the range of 362 % to 511 %. Moreover, a decay in Shore A hardness from 35.8 to 30.1 was recognized with increased porosity as well, which conforms to the alleged trend by Zare et al. [38].

As observed from the Young's modulus, the foams produced were up to 78.11 % more flexible than the silicone formulation synthesized by Lim et al. [23], which had a reported value of 1.69 MPa. The hardness values were up to 39.8 % lower than the conventional Silastic silicone formulation with Shore A of 50 [39]. This deduced that the amount of porogen introduced is a manipulated variable which significantly affects the pore properties and subsequently mechanical properties of the silicone foam [40]. Hence, the viability of the direct templating method to produce silicone foam with tuneable mechanical properties was demonstrated.

Table 3 *Mechanical properties of foams with various glucose content*

Glucose content (phr)	Young's modulus (MPa)	Ultimate tensile strength (MPa)	Elongation at break (%)	Hardness (shore A)
15	0.50	0.96	511	35.8
35	0.43	0.76	427	34.5
55	0.37	0.59	362	30.1

3.4 Three-Dimensional Printed Silicone Structures

Fig. 6 demonstrates the printability of the glucose/PDMS inks. The printed articles are representative for all inks with different glucose content. The printability of the inks was attributed to their satisfactory rheological properties in Table 1. Firstly, all inks featured solid-like properties in the linear viscoelastic region, as their loss factors were 0.46 to 0.37 (tan δ <1). Next, the viscosities at the printing shear rate used of 62.41 Pa·s to 109.66 Pa·s were still relatively low. The torque provided by the stepper motor was sufficient to drive the lead-screw for

smooth material extrusion, proven by the absence of under-extrusion. The static yield stress values of 120.04 Pa to 135.68 Pa were high enough to maintain the stacking of layers, as the structures did not crumple during printing, while the storage moduli varied from 4596.03 Pa to 12932.23 Pa. These values satisfy the rheological parameters required for DIW as mentioned under Section 3.1, and were adequate to maintain shape retention during printing, exemplified by the scaffolding which portrayed intricate details. In brief, the addition of glucose particles did not diminish the thixotropic characteristics of the RTV-1 silicone ink formulation, which allowed for successful printing.

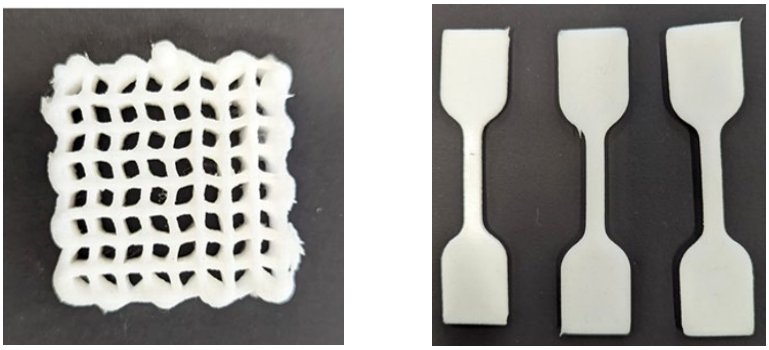

(a) **(b)**

Fig. 6 *Successful printing of PDMS/glucose ink samples as (a) Scaffold; (b) Tensile bars*

4. Conclusions

In short, the developed porous silicone foams via direct templating can be 3D printed even to the precise geometry of a scaffold structure via DIW. The templating approach was cost-effective and not hazardous, with glucose crystals chosen as the template, while deionized water was the solvent of choice. It was discernible that 3D silicone structure with tuneable pores and mechanical properties while maintaining the printability criteria can be realized under the feasible glucose content range of 15 phr to 55 phr. The average pore sizes and porosity are evidenced to be linearly correlated to the glucose content, while the mechanical properties were reliant on the resulting porosity.

Acknowledgement

The research was supported by the Ministry of Higher Education (MoHE), through the Fundamental Research Grant Scheme (FRGS/1/2023/TK10/UTAR/02/1).

Conflict of Interest

Authors declare that there is no conflict of interests regarding the publication of the paper.

Author Contribution

The authors confirm contribution to the paper as follows: ***study conception and design:*** *Kenrick Weiting Tie, Purani Mohana Sundaram, Jia Huey Sim, Jing Yuen Tey;* ***data collection:*** *Kenrick Weiting Tie, Purani Mohana Sundaram;* ***analysis and interpretation of results:*** *Kenrick Weiting Tie, Purani Mohana Sundaram;* ***draft manuscript preparation:*** *Kenrick Weiting Tie, Purani Mohana Sundaram, Jia Huey Sim, Zhi Hua Lee, Law Yong Ng, Wei Hong Yeo. All authors reviewed the results and approved the final version of the manuscript.*

References

[1] Mina Zare, Erfan Rezvani Ghomi, Prabhuraj D. Venkatraman & Seeram Ramakrishna (2021) Silicone-based biomaterials for biomedical applications: Antimicrobial strategies and 3D printing technologies, *Journal of Applied Polymer Science*, *138(38)*, 50969, https://doi.org/10.1002/app.50969

[2] Subhas C. Shit & Pathik Shah (2013) A review on silicone rubber, *National Academy Science Letters*, *36*, 355-365, https://doi.org/10.1007/s40009-013-0150-2

[3] Aslan Miriyev, Boxi Xia, Jacob Carroll Joseph & Hod Lipson (2019) Additive Manufacturing of Silicone Composites for Soft Actuation, *3D Printing and Additive Manufacturing*, *6(6)*, 309-318, https://doi.org/10.1089/3dp.2019.0116

[4] Piotr Mazurek, Sindhu Vudayagiri & Anne Ladegaard Skov (2019) How to tailor flexible silicone elastomers with mechanical integrity: A tutorial review. *The Royal Society of Chemistry, 48(6)*, 1448-1464, https://doi.org/10.1039/C8CS00963E

[5] Qiyi Chen, Jiayu Zhao, Jingbo Ren, Lihan Rong, Peng-Fei Cao & Rigoberto C. Advincula (2019) 3D Printed multifunctional, hyperelastic silicone rubber foam, *Advanced Functional Materials*, *29(23)*, 1900469, https://doi.org/10.1002/adfm.201900469

[6] Soumaya Berro, Ranim El Ahdab, Houssein Hajj Hassan, Hassan M. Khachfe & Mohamad Hajj-Hassan (2015), From plastic to silicone: The novelties in porous polymer fabrications, *Journal of Nanomaterials*, *2015(1)*, 142195, https://doi.org/10.1155/2015/142195

[7] Andres Diaz Lantada, Hernan Alarcon Iniesta, Beatriz Pareja Sanchez & Josefa Predestinación García-Ruíz (2014) Free-form rapid prototyped porous PDMS scaffolds incorporating growth factors promote chondrogenesis, *Advances in Materials Science and Engineering*, *2014(1)*, 612976, https://doi.org/10.1155/2014/612976

[8] Subin Kang, Jaehong Lee, Sanggeun Lee, SeulGee Kim, Jae-Kang Kim, Hassan Algadi, Saleh Al-Sayari, Dae-Eun Kim, DaeEun Kim & Taeyoon Lee (2016) Highly sensitive pressure sensor based on bioinspired porous structure for real-time tactile sensing, *Advanced Electronic Materials*, *2(12)*, 1600356, https://doi.org/10.1002/aelm.201600356

[9] Juwon Hwang, Yeongjun Kim, Hyeondong Yang & Je Hoon Oh (2021) Fabrication of hierarchically porous structured PDMS composites and their application as a flexible capacitive pressure sensor, *Composites Part B: Engineering*, *211*, 108607, https://doi.org/10.1016/j.compositesb.2021.108607

[10] Elham Davoodi, Hossein Montazerian, Reihaneh Haghniaz, Armin Rashidi, Samad Ahadian, Amir Sheikhi, Jun Chen, Ali KhademhosseiniAbbas S. MilaniMina Hoorfar & Ehsan Toyserkani (2020) 3D-printed ultra-robust surface-doped porous silicone sensors for wearable biomonitoring. *ACS Nano*, *14(2)*, 1520-1532, https://doi.org/10.1021/acsnano.9b06283

[11] Thibaud Métivier & Philippe Cassagnau (2019) New trends in cellular silicone: Innovations and applications, *Journal of Cellular Plastics*, *55(2)*, 151-200, https://doi.org/10.1177/0021955X18806845

[12] P. Mazurek, B. E. F. Ekbrant, F. B. Madsen, L. Yu & A. L. Skov (2019) Glycerol-silicone foams – Tunable 3-phase elastomeric porous materials, *European Polymer Journal*, *113*, 107-114, https://doi.org/10.1016/j.eurpolymj.2019.01.051

[13] José González-Rivera, Rossella Iglio, Giuseppe Barillaro, Celia Duce & Maria Rosaria Tinè (2018) Structural and thermoanalytical characterization of 3D porous PDMS foam materials: The effect of impurities derived from a sugar templating process, *Polymers*, *10(6)*, 616, https://doi.org/10.3390/polym10060616

[14] Wenbo Liu, Ronald R. Campbell, Mookkan Periyasamy & Michael A. Hickner (2022) Additive manufacturing of silicone-thermoplastic elastomeric composite architectures, *Journal of Composite Materials*, *56(29)*, 4409-4419, https://doi.org/10.1177/00219983221131614

[15] Changyong Liu, Ninggui Huang, Feng Xu, Junda Tong, Zhangwei Chen, Xuchun Gui, Yuelong Fu & Changshi Lao (2018) 3D printing technologies for flexible tactile sensors toward wearable electronics and electronic skin, *Polymers, 10(6)*, 1-31, https://doi.org/10.3390/polym10060629

[16] Rebekah Woo, Grace Chen, Jiayu Zhao & Jinhye Bae (2021). Structure-mechanical property relationships of 3D-printed porous polydimethylsiloxane, *ACS Applied Polymer Materials*, *3(7)*, 3496-3503, https://doi.org/10.1021/acsapm.1c00417

[17] Daniel A. Rau, Christopher B. Williams & Michael J. Bortner (2023) Progress in materials science rheology and printability: A survey of critical relationships for direct ink writes materials design, *Progress in Materials Science*, *140*, 101188, https://doi.org/10.1016/j.pmatsci.2023.101188

[18] Amin M'barki, Lydéric Bocquet & Adam Stevenson (2017) Linking rheology and printability for dense and strong ceramics by direct ink writing, *Scientific Reports*, *7*, 6017, https://doi.org/10.1038/s41598-017-06115-0

[19] Mohammad Abshirini, Mrinal C. Saha, Laura Cummings & Thomas Robison (2021) Synthesis and characterization of porous polydimethylsiloxane structures with adjustable porosity and pore morphology using emulsion templating technique, *Polymer Engineering and Science, 61(7)*, 1943-1955, https://doi.org/10.1002/pen.25710

[20] Xin-Yi Teoh, Bin Zhang, Peter Belton, Siok-Yee Chan & Sheng Qi (2022) The effects of solid particle containing inks on the printing quality of porous pharmaceutical structures fabricated by 3D semi-solid extrusion printing, *Pharmaceutical Research*, *39*, 1267-1279,

https://doi.org/10.1007/s11095-022-03299-7

[21] Maria Victoria Alcantar Umaran & Ruben Labandera Menchavez (2013) Aqueous dispersion of red clay-based ceramic powder with the addition of starch, *Materials Research*, *16(2)*, 375-384, https://doi.org/10.1590/S1516-14392013005000002

[22] Mohammad A. Azad, Deborah Olawuni, Georgia Kimbell, Abu Zayed Md Badruddoza, Md Shahadat Hossain & Tasnim Sultana (2020) Polymers for extrusion-based 3D printing of pharmaceuticals: A holistic materials – process perspective, *Pharmaceutics*, *12(2)*, 124, https://doi.org/10.3390/pharmaceutics12020124

[23] Jeng Jit Lim, Jia Huey Sim & Jing Yuen Tey (2023) Rheological formulation of room temperature vulcanizing silicone elastomer ink for extrusion-based 3D printing at room temperature, *Journal of Manufacturing Processes*, *102*, 632-643, https://doi.org/10.1016/j.jmapro.2023.07.066

[24] D. ASTM (2015) Standard test method for determining the rheological properties of asphalt binder using a dynamic shear rheometer, *ASTM International West Conshohocken, PA*.

https://www.astm.org/d7175-23.html

[25] Yiliang Cheng, Hantang Qin, Nuria C. Acevedo, Xuepeng Jiang & Xiaolei Shi. (2020) 3D printing of extended-release tablets of theophylline using hydroxypropyl methylcellulose (HPMC) hydrogels, *International Journal of Pharmaceutics*, *591*, 119983, https://doi.org/10.1016/j.ijpharm.2020.119983

[26] Marko Bek, Joamin Gonzalez-Gutierrez, Christian Kukla, Klementina Pušnik Črešnar, Boris Maroh & Lidija Slemenik Perše (2020) Rheological behaviour of highly filled materials for injection moulding and additive manufacturing: Effect of particle material and loading, *Applied Sciences*, *10(22)*, 7993, https://doi.org/10.3390/app10227993

[27] Zhenhua Tang, Shuhai Jia, Xuesong Shi, Bo Li & Chenghao Zhou (2019) Coaxial printing of silicone elastomer composite fibers for stretchable and wearable piezoresistive sensors, *Polymers*, *11(4)*, 666, https://doi.org/10.3390/polym11040666

[28] Enze Liao, Yaling Zhang, Yu Su, Chenyang Zhang, Chengzhen Geng, Changlin Li, Xiaoyan Liu, Yu Liu & Ai Lu (2024) Active mixing of two-component viscoelastic silicone ink at molecular level for spatiotemporally controlled 3D/4D printing of cellular silicones, *Polymer*, *302*, 127053, https://doi.org/10.1016/j.polymer.2024.127053

[29] Peiran Wei, Ciera Cipriani, Chia-Min Hsieh, Krutarth Kamani, Simon Rogers & Emily Pentzer (2023) Go with the flow: Rheological requirements for direct ink write printability, *Journal of Applied Physics*, *134*, 100701, https://doi.org/10.1063/5.0155896

[30] Zhiyang Lyu, J. Justin Koh, Gwendolyn JH Lim, Danwei Zhang, Ting Xiong, Lei Zhang, Siqi Liu, Junfei Duan, Jun Ding, John Wang, Jinlan Wang, Yunfei Chen & Chaobin He (2022) Direct ink writing of programmable functional silicone-based composites for 4D printing applications, *Interdisciplinary Materials*, *1(4)*, 507-516, https://doi.org/10.1002/idm2.12027

[31] Clément Perrinet, Edwin-Joffrey Courtial, Arthur Colly, Christophe Marquette & René Fulchiron (2020) An emulsion approach to resolve the paradox of 3D printing of very soft silicones, *Advanced Materials Technologies*, *5(6)*, 1-9, https://doi.org/10.1002/admt.201901080

[32] Patrick Wilms, Jörg Hinrichs & Reinhard Kohlus (2022) Macroscopic rheology of non - Brownian suspensions at high shear rates: The influence of solid volume fraction and non - Newtonian behaviour of the liquid phase, *Rheologica Acta*, *61*, 123-138, https://doi.org/10.1007/s00397-021-01320-1

[33] Rowan W. Sanderson, Qi Fang, Andrea Curatolo, Wayne Adams, Devina D. Lakhiani, Hina M. Ismail, Ken Y. Foo, Benjamin F. Dessauvagie, Bruce Latham, Chris Yeomans, Christobel M. Saunders & Brendan F. Kennedy (2020) Camera-based optical palpation, *Scientific Reports*, *10(1)*, 15951, https://doi.org/10.1038/s41598-020-72603-5

[34] Kritika Pandey, Harsimran Singh Bindra, Debarati Paul & Ranu Nayak (2020) Smart multi-tasking PDMS Nanocomposite sponges for microbial and oil contamination removal from water, *Journal of Polymer Research*, *27(7)*, 189, https://doi.org/10.1007/s10965-020-02109-1

[35] Nasim Annabi, Jason W. Nichol, Xia Zhong, Chengdong Ji, Sandeep Koshy, Ali Khademhosseini & Fariba Dehghani (2010) Controlling the porosity and microarchitecture of hydrogels for tissue engineering, *Tissue Engineering: Part B*, *16(4)*, 371-383, https://doi.org/10.1089/ten.teb.2009.0639

[36] E. M. Prieto & S. A. Guelcher (2014) Tailoring properties of polymeric biomedical foams, In P. A. Netti (Ed.), *Biomedical Foams for Tissue Engineering Applications* (pp. 129-162). Woodhead Publishing Limited. https://doi.org/10.1533/9780857097033.1.129

[37] Junhui Si, Zhixiang Cui, Peng Xie, Lairui Song, Qianting Wang, Qiong Liu & Chuntai Liu (2016) Characterization of 3D elastic porous polydimethylsiloxane (PDMS) cell scaffolds fabricated by VARTM and particle leaching, *Journal of Applied Polymer Science*, *133(4)*, 1-9, https://doi.org/10.1002/app.42909

[38] Longgui Peng, Lei Lei, Yongqiang Liu & Lifei Du (2021) Improved mechanical and sound absorption properties of open cell silicone rubber foam with NaCl as the pore-forming agent, *Materials*, *14*, 195, https://doi.org/10.3390/ma14010195

[39] Veronika M. Miron, Sebastian Lämmermann, Umut Çakmak, and Zoltán Major (2021) Material Characterization of 3D-printed Silicone Elastomers, *Procedia Structural Integrity*, *34*, 65-70, https://doi.org/10.1016/j.prostr.2021.12.010

[40] Siti Khadijah Ab Rahman, Nor Azah Yusof, Abdul Halim Abdullah, Faruq Mohammad, Azni Idris & Hamad A. Al-Lohedan (2018) Evaluation of porogen factors for the preparation of ion imprinted polymer monoliths used in mercury removal, *PLoS ONE*, *13(4)*, e0195546, https://doi.org/10.1371/journal.pone.0195546